White Rose Research Online

eprints@whiterose.ac.uk
https://eprints.whiterose.ac.uk
Universities of Leeds, Sheffield and York

Deposited via The University of Sheffield.

White Rose Research Online URL for this paper:
https://eprints.whiterose.ac.uk/id/eprint/166548/

Version: Published Version

Article:
Tsap, Y., Fedun, V., Cheremnykh, O. et al. (2020) On the stabilization of a twisted magnetic flux tube. The Astrophysical Journal, 901 (2).

https://doi.org/10.3847/1538-4357/abaf01

Reuse
This article is distributed under the terms of the Creative Commons Attribution (CC BY) licence. This licence allows you to distribute, remix, tweak, and build upon the work, even commercially, as long as you credit the authors for the original work. More information and the full terms of the licence here:
https://creativecommons.org/licenses/

Takedown
If you consider content in White Rose Research Online to be in breach of UK law, please notify us by emailing eprints@whiterose.ac.uk including the URL of the record and the reason for the withdrawal request.

UNIVERSITY OF LEEDS
University of Sheffield
UNIVERSITY of York

The Astrophysical Journal, 901:99 (9pp), 2020 October 1 https://doi.org/10.3847/1538-4357/abaf01
© 2020. The Author(s). Published by the American Astronomical Society.
OPEN ACCESS

On the Stabilization of a Twisted Magnetic Flux Tube

Yuriy Tsap[1,5], Viktor Fedun[2], Oleg Cheremnykh[3], Alexander Stepanov[4], Alexandr Kryshtal[3], and Yulia Kopylova[4]
[1] Crimean Astrophysical Observatory, Crimea, Nauchny, 298409; yuratsap2001@gmail.com
[2] Plasma Dynamics Group, Department of Automatic Control and Systems Engineering, The University of Sheffield, Mappin Street, Sheffield, S1 3JD, UK
[3] Space Research Institute, Kiev, 03680, 187, Ukraine
[4] Central Astronomical Observatory at Pulkovo, St. Petersburg, 196140, Russia
Received 2020 May 8; revised 2020 July 14; accepted 2020 July 21; published 2020 September 25

Abstract

The linear magnetohydrodynamic stability of a shielding magnetic flux rope with a surface current under coronal solar conditions is analyzed in the framework of an energy principle. The equation describing the potential energy change induced by disturbances of the equilibrium was derived. It has been shown that the surface reverse current shielding the azimuthal component of the magnetic field lines outside a flux rope stabilizes the development of kink- and flute-type instabilities in the long-wavelength limit independently of the cross-sectional radial profile of current density. Kink modes are the most unstable ones as their generation requires less energy than other modes. Based on the obtained dispersion relation for kink oscillations, we proposed a new expression for the determination of magnetic field components of the twisted loop.

Unified Astronomy Thesaurus concepts: Magnetohydrodynamics (1964); Space plasmas (1544)

1. Introduction

The magnetic flux tube and current sheets are the main "building blocks" of solar magnetic configurations (see, e.g., Parker 1979; Priest 1984; Priest & Forbes 2000; Ryutova 2018). The magnetohydrodynamic (MHD) instabilities of magnetic flux ropes (i.e., twisted flux tubes) are partially responsible for plasma heating, particle acceleration, and wave generation at different spatio-temporal scales. Kink instability is a subject of special interest since there is much evidence that this instability can be responsible for flare energy release and coronal mass ejections (see, e.g., Sakurai 1976; Török & Kliem 2005; Myers et al. 2015; Chen 2017). However, the question about the stability conditions of flux ropes is not fully resolved yet (see, e.g., Priest 1984; Hassanin et al. 2016).

Previously, the kink instability of a plasma cylinder with a longitudinal electric current was investigated theoretically by Kruskal & Schwarzschild (1954) and Leontovich & Shafranov (1961). It has been shown that a flux rope with length L, radius a, and azimuthal and longitudinal magnetic field components B_φ and B_z, respectively, becomes unstable with respect to kink perturbations if the total twist angle of magnetic field lines $\Phi = LB_\varphi(a)/aB_z(a)$ exceeds some critical value $\Phi_c = 2\pi$. This value corresponds only to one full rotation of the magnetic field line. For solar coronal loops, which we can consider as straight cylinders, the aspect ratio $a/L \ll 1$ (see, e.g., Nakariakov et al. 1999), and therefore the azimuthal component of magnetic field B_φ, is $B_\varphi \ll B_z$. Although the Kruskal–Schafranov condition has been obtained for a flux rope with an electric current surrounded by vacuum, with an accuracy of the coefficient the critical twist angle ($\Phi_c = 2.9\pi$) is still valid for solar coronal loops anchored at footpoints (see, e.g., Hood & Priest 1981; Priest 1984). Meanwhile, Srivastava et al. (2010) have found the signature of a highly twisted coronal loop in the active region by using satellite multiwavelength observations. The observed coronal loop showed a strong right-handed twist in the chromospheric and coronal images with a total twist angle for the whole loop $\Phi \sim 12\pi$. In turn, Liu et al. (2019), based on the study of twist angles of magnetic field lines released by 30 off-limb rotational solar coronal jets, has found that the maximum $\Phi \approx 9.4\pi$ and that the kink instability threshold in the solar atmosphere should not be a constant.

A number of theoretical studies have shown that magnetic flux tubes are responsible for the variety of observable solar phenomena that should be isolated in the photosphere, i.e., they are surrounded by the field-free plasma (see, e.g., Ryutov & Ryutova 1976; Parker 1979; Spruit 1981; Priest 1984; Fan 2009; Weber & Browning 2016; Tsap et al. 2018). Parker (1996) has shown that the total current across a cross section of the photospheric magnetic flux tube is equal to zero due to the presence of the surface current. In particular, this suggests that the presence of nonvanishing vertical currents is an artifact caused by the limited spatial resolution of the observing magnetograph. In contrast, Melrose (1991, 1995, 1996) has found arguments against these representations. Some observational and numerical simulation results show evidence in favor of nonneutralized electric currents in the active regions of the solar photosphere (see, e.g., Georgoulis 2018; Schmieder & Aulanier 2018; Russell et al. 2019). At the same time, we cannot exclude the fact that partially isolated magnetic flux ropes with a shielding longitudinal surface current also exist (see also Wilkinson et al. 1992; Wheatland 2000; Schmieder & Aulanier 2018).

Sakurai (1976) has applied the method of normal modes to analyze the kink stability of a filament (an isolated twisted magnetic flux tube). However, the external magnetic field and gas pressure were not considered. Linton et al. (1996) have taken into account the external gas pressure and studied the linear stability of an isolated flux rope below the solar photosphere within the linear approximation. Based on an energy principle the authors concluded that kink instability

[5] While the AAS journals adhere to and respect UN resolutions regarding the designations of territories (available at http://www.un.org/press/en), it is our policy to use the affiliations provided by our authors on published articles.

Original content from this work may be used under the terms of the Creative Commons Attribution 4.0 licence. Any further distribution of this work must maintain attribution to the author(s) and the title of the work, journal citation and DOI.

consists mainly of internal motions while the helical translations of the entire tube are stable. It was suggested that the plasma $\beta \gg 1$ which is unusual in the lower solar corona. The partially isolated magnetic flux ropes with oppositely directed volume currents were studied previously by Mikic et al. (1990). By using numerical calculations, it was shown that the magnetic flux rope becomes unstable if the twist angle $\Phi > 4.8\pi$. Recently, Cheremnykh et al. (2017) have studied incompressible perturbations by using the normal modes method. It was found that in the long-wavelength limit the eigenfrequency of the kink mode ($m = 1$) is real and completely unaffected by the choice of internal background magnetic twist. Later, Cheremnykh et al. (2018) showed that the stability criterion of the $m = 1$ mode is independent of the background azimuthal components of the plasma velocity and magnetic field. The results of studies mentioned above show that the reverse current inside a flux rope should stabilize the development of kink instability. However, the proposed approaches had some essential restrictions associated with the mathematical difficulties caused by the complexity of either the magnetic configuration (Mikic et al. 1990; Linton et al. 1996) or calculation methodologies (Cheremnykh et al. 2017).

The main aim of this work is to investigate the stability of the partially isolated magnetic flux rope with a shielding surface current under solar coronal conditions on the basis of an energy principle (Bernstein et al. 1958). This method has been used previously for theoretical investigation of the solar coronal loops (e.g., Priest 1984; Hood 1986; Melville et al. 1986; Linton et al. 1996) but shielding longitudinal currents had not been considered.

The paper is organized as follows. In Section 2, we present the main idea of our approach. The procedure of minimization of the potential energy change and the search of the eigenfunctions of a flux rope are described in Section 3 and Section 4, respectively. Section 5 is devoted to the analysis of the stability of kink modes and application of obtained theoretical results. Discussions and conclusions are provided in Section 6.

2. An Energy Principle for a Flux Rope with Sharp Boundary

In the cgs system of units the equation of plasma motion, induction equation, continuity, and energy balance in a single-fluid ideal MHD can be represented as

$$\rho\frac{d\boldsymbol{v}}{dt} = -\nabla p + \frac{\boldsymbol{j}\times\boldsymbol{B}}{c} + \rho\boldsymbol{g}, \tag{1}$$

$$\frac{\partial \boldsymbol{B}}{\partial t} = \nabla\times[\boldsymbol{v}\times\boldsymbol{B}], \tag{2}$$

$$\frac{\partial \rho}{\partial t} + \nabla(\rho\boldsymbol{v}) = 0, \tag{3}$$

$$\frac{d}{dt}\left(\frac{p}{\rho^{\gamma}}\right) = 0, \tag{4}$$

where ρ is the plasma mass density, $\boldsymbol{v}$ is the plasma velocity, p is the gas pressure, $\boldsymbol{g}$ is the the acceleration of gravity, $\gamma = 5/3$ is the ratio of specific heat, and the electric current density

$$\boldsymbol{j} = \frac{c}{4\pi}\nabla\times\boldsymbol{B}. \tag{5}$$

Let $\boldsymbol{S}$ be the displacement vector of the elementary plasma volume from the equilibrium. Then, taking into account the equilibrium equation

$$-\nabla p + \frac{\boldsymbol{j}\times\boldsymbol{B}}{c} + \rho\boldsymbol{g} = 0, \tag{6}$$

as well as Equations (2)–(5), the linearized Equation (1) can be written as (see, e.g., Bernstein et al. 1958):

$$\rho\ddot{\boldsymbol{S}} + \hat{\boldsymbol{K}}\{\boldsymbol{S}\} = 0. \tag{7}$$

Here, the differential operator $\hat{\boldsymbol{K}}$ depends on the equilibrium values of the gas pressure p, plasma density ρ, and magnetic field $\boldsymbol{B}$:

$$\begin{aligned}\hat{\boldsymbol{K}}\{\boldsymbol{S}\} = {} & \frac{1}{4\pi}[\nabla\times[\nabla\times(\boldsymbol{S}\times\boldsymbol{B})]]\\ & \times\boldsymbol{B} + \frac{1}{c}\boldsymbol{j}\times[\nabla\times(\boldsymbol{S}\times\boldsymbol{B})]\\ & + \nabla[(\boldsymbol{S}\nabla)p + \gamma p\,\nabla\boldsymbol{S}] - \boldsymbol{g}\,\nabla(\rho\boldsymbol{S}),\end{aligned} \tag{8}$$

where

$$\ddot{\boldsymbol{S}} = \frac{\partial\boldsymbol{v}}{\partial t} = \frac{\partial^2\boldsymbol{S}}{\partial t^2}.$$

Bernstein et al. (1958) have shown that the differential operator $\hat{\boldsymbol{K}}$ is Hermitian, i.e., the following equality should be satisfied

$$\int\boldsymbol{\eta}\hat{\boldsymbol{K}}\{\boldsymbol{\xi}\}dV = \int\boldsymbol{\xi}\hat{\boldsymbol{K}}\{\boldsymbol{\eta}\}dV, \tag{9}$$

for the arbitrary eigenfunctions $\boldsymbol{\eta}$ and $\boldsymbol{\xi}$.

By multiplying Equation (7) in a scalar way by the time derivative of the vector displacement $\dot{\boldsymbol{S}}$ and by integrating it over the plasma volume V, together with Equation (9), we arrive at

$$\frac{\partial}{\partial t}\left[\frac{1}{2}\int_V\rho\dot{\boldsymbol{S}}^2dV + \frac{1}{2}\int_V\boldsymbol{S}\hat{\boldsymbol{K}}\{\boldsymbol{S}\}dV\right] = 0,$$

or

$$T + W = \text{const}, \tag{10}$$

where changes in kinetic T and potential W energies are

$$T = \frac{1}{2}\int_V\rho\dot{\boldsymbol{S}}^2dV, \quad W = \frac{1}{2}\int_V\boldsymbol{S}\hat{\boldsymbol{K}}\{\boldsymbol{S}\}dV.$$

The equation of energy conservation (10) shows that any arbitrary perturbation, with a decrease of potential energy ($W < 0$), leads to the increase of kinetic energy T and, therefore, to the development of MHD instability. In contrast, the system is stable if a change of energy $W > 0$. This is the main idea of an energy principle (see also Sakurai 1976). Such an approach allows us to obtain useful information about stability conditions without the consideration of eigenfunction $\boldsymbol{S}$ in detail.

By assuming that $\boldsymbol{S}$ can be represented as

$$\boldsymbol{S}(\boldsymbol{r}, t) = \boldsymbol{s}(\boldsymbol{r})\exp(i\Omega t),$$

instead of Equation (7) we have

$$\lambda\rho\boldsymbol{s} = \hat{\boldsymbol{K}}\{\boldsymbol{s}\}, \quad \lambda = \Omega^2. \tag{11}$$

Therefore, the problem of MHD stability focuses on finding the eigenvalues λ. Equation (9) suggests that the eigenvalues λ

should be real. The negative eigenvalues of λ correspond to the instability growth rate $\Gamma = \sqrt{|\lambda|}$ while the positive ones describe the frequency $\Omega = \sqrt{\lambda}$ of MHD eigenmodes. Investigation of the MHD stability of magnetic plasma configurations reduces to the finding of eigenvalues λ of the linear differential operator $\hat{\boldsymbol{K}}$.

The vector $\boldsymbol{s}$ can be found analytically for a few limited cases by using the method of normal modes (e.g., Priest 1984; Goedbloed & Poedts 2004). Therefore, an energy principle is more convenient for the analysis of instability conditions.

By multiplying Equation (11) by $\boldsymbol{s}$ and integrating over the plasma volume, we can find the eigenvalues as

$$\lambda = \frac{2W}{\int_V \rho \boldsymbol{s}^2 dV}. \tag{12}$$

From Equation (12), it follows that smallest positive eigenvalues λ correspond to the most feasible oscillations. These eigenvalues can be identified by applying the Rayleigh–Ritz method (see, e.g., Dungey 2016).

For the sharp plasma–plasma boundary which separates internal (i) and external (e) regions by surface σ, from Equation (12) we have (Tsap et al. 2006, 2008)

$$\lambda = 2\frac{W_i + W_e + W_\sigma}{\int_{V_i} \rho \boldsymbol{s}^2 dV + \int_{V_e} \rho \boldsymbol{s}^2 dV}. \tag{13}$$

Here

$$W_i = \frac{1}{2}\int_{V_i} K\, dV, \quad W_e = \frac{1}{2}\int_{V_e} K\, dV,$$
$$W_\sigma = \frac{1}{2}\oint_\sigma \frac{d\langle P\rangle}{dn} s_n^2(\boldsymbol{r})\, d\sigma, \tag{14}$$

$$K = \frac{\delta B^2}{4\pi} + \frac{\boldsymbol{j}}{c}(\boldsymbol{s} \times \boldsymbol{\delta B}) - \delta p \nabla \boldsymbol{s} + \boldsymbol{g}\boldsymbol{s}\nabla(\rho \boldsymbol{s}), \tag{15}$$

$$\delta \boldsymbol{B} = \nabla \times (\boldsymbol{s} \times \boldsymbol{B}), \quad P = p + \frac{B^2}{8\pi}, \quad \langle P\rangle = P_e - P_i,$$

$$\delta p = -(\boldsymbol{s}\nabla p) - \gamma p(\nabla \boldsymbol{s}), \quad s_n = \boldsymbol{s}\boldsymbol{n}, \frac{d}{dn} = \boldsymbol{n}\nabla,$$

where $\boldsymbol{n}$ is the normal to the boundary surface σ. The equation of the pressure balance should be satisfied at the boundary surface σ

$$\left(p_i + \frac{B_i^2}{8\pi}\right)_\sigma = \left(p_e + \frac{B_e^2}{8\pi}\right)_\sigma. \tag{16}$$

By neglecting gravity, from Equation (15) for K we can conclude that the main source of instability is the electric current $\boldsymbol{j}$ (Ampere force) since terms with the gas pressure p should be equal to zero for the most critical modes. Indeed, the vector $\boldsymbol{s}$ can be expressed in terms of longitudinal $\boldsymbol{s}_\parallel$ and perpendicular $\boldsymbol{s}_\perp$ components in respect to the direction of magnetic field $\boldsymbol{B}$

$$\boldsymbol{s} = \boldsymbol{s}_\parallel + \boldsymbol{s}_\perp.$$

As a result, is easy to show (see, e.g., Zagorodny & Cheremnykh 2014) that $\boldsymbol{s}_\parallel$ is only present in the term

$$\gamma p(\nabla \boldsymbol{s})^2 = \gamma p(\nabla \boldsymbol{s}_\parallel + \nabla \boldsymbol{s}_\perp)^2.$$

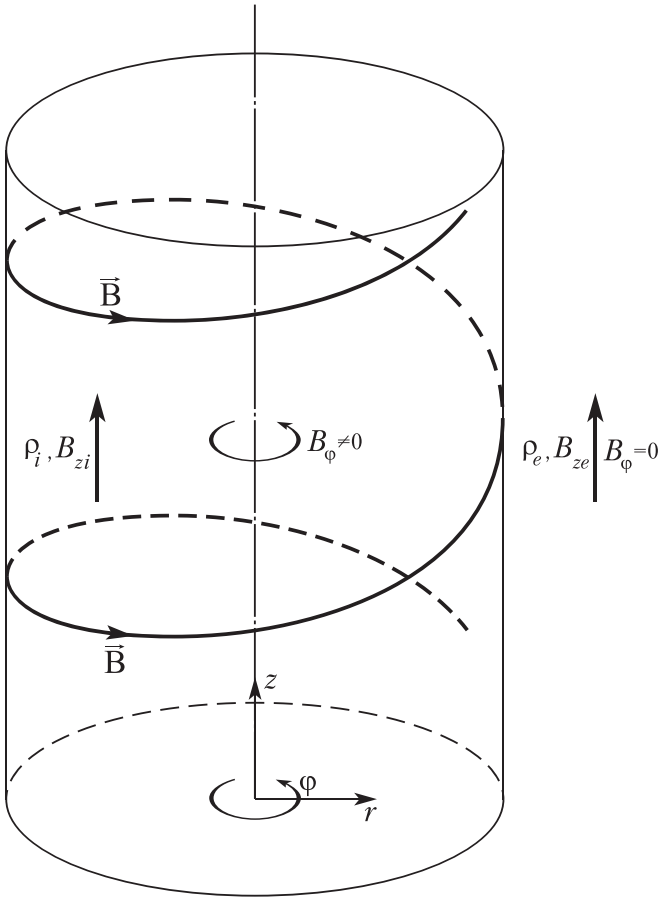

Figure 1. Sketch of a shielding magnetic flux rope with an internal surface current.

The incompressible perturbations are most unstable when the values of W_i and W_e in Equation (14) are minimal, i.e., when $\nabla \boldsymbol{s} = 0$. It can be achieved by choosing $\boldsymbol{s}_\parallel$.

By using a cylindrical coordinate system (r, φ, z), let us consider a magnetic flux rope with a shielding surface current (Figure 1). The proposed model suggests that the equilibrium magnetic field is

$$\boldsymbol{B} = \begin{cases} (0, B_\varphi(r), B_{zi}(r)), & r \leqslant a; \\ (0, 0, B_{ze}), & r > a. \end{cases} \tag{17}$$

As it follows from expression (17) we consider the cylinder boundary as an MHD discontinuity with a surface current. Note that the proposed model reduces to a partially isolated flux rope because the azimuthal component of the magnetic field B_φ is equal to zero outside of the tube.

In our study we take into account the surface potential energy W_σ, which is usually not considered in a laboratory plasma. By neglecting gravity, Equations (5) and (6) give:

$$\nabla\left(p + \frac{B^2}{8\pi}\right) = \frac{1}{4\pi}(\boldsymbol{B}\nabla)\boldsymbol{B}.$$

Therefore, for the equation of equilibrium in the r-direction we have

$$\frac{dP}{dr} = -\frac{B_\varphi^2}{4\pi r}. \tag{18}$$

According to the Equations (15) and (18) the derivative of $\langle P\rangle$ is

$$\frac{d\langle P\rangle}{dn} = \frac{dP_e}{dr} - \frac{dP_i}{dr} = \frac{B_\varphi^2}{4\pi r}. \quad (19)$$

The displacement $\boldsymbol{s}$ can be represented as

$$\boldsymbol{s}(\boldsymbol{r}) = \boldsymbol{s}(r)e^{i(m\varphi+kz)}, \quad (20)$$

where the integer number m describes the sausage ($m = 0$), kink ($m = 1$), and fluting ($m \geqslant 2$) modes. By setting the wavenumber k as $k = -2\pi n/L$, where $n \geqslant 1$ is an integer number, the element of the lateral surface of the magnetic cylinder $d\sigma$ as

$$d\sigma = ad\varphi dL,$$

and substituting Equations (19) and (20) into Equation (14), we obtain

$$W_\sigma = \frac{1}{2}\int_0^{2\pi}\int_0^L \frac{B_\varphi^2(a)}{4\pi}s_r^2(a, \varphi, z)dzd\varphi = L\frac{B_\varphi^2(a)}{8}s_r^2(a). \quad (21)$$

Since $W_\sigma > 0$, the surface longitudinal currents stabilize the development of MHD instabilities. Moreover, stabilization depends on the value of the azimuthal component of the magnetic field $B_\varphi(r)$ at the boundary only.

3. Minimization of W_i and W_e Energies for a Flux Rope

The condition $\nabla\boldsymbol{s} = 0$ allows us to minimize the potential energies over the internal V_i and external V_e volumes in respect to s_φ and s_z. By using the equation for a perturbed magnetic field

$$\delta\boldsymbol{B} = \nabla \times [\boldsymbol{s} \times \boldsymbol{B}],$$

which follows from the induction Equation (2), and Equation (20), we arrive at

$$\begin{aligned}\delta B_r &= i(\boldsymbol{kB})s_r,\\ \delta B_\varphi &= ik\zeta - \frac{d}{dr}(s_r B_\varphi),\\ \delta B_z &= -\frac{im\zeta}{r} - \frac{1}{r}\frac{d}{dr}(rs_r B_z),\end{aligned} \quad (22)$$

where

$$\boldsymbol{kB} = \frac{m}{r}B_\varphi + kB_z, \quad \zeta = s_\varphi B_z - s_z B_\varphi. \quad (23)$$

In turn, in cylindrical coordinates, $\nabla\boldsymbol{s} = 0$ reduces to

$$\frac{1}{r}\frac{\partial}{\partial r}(rs_r) + \frac{im}{r}s_\varphi + iks_z = 0. \quad (24)$$

By combining Equations (23) and (24), we can express the displacements s_φ and s_z in terms of s_r and ζ as

$$\begin{aligned}i(\boldsymbol{kB})s_\varphi &= ik\zeta - \frac{B_\varphi}{r}\frac{d}{dr}(rs_r),\\ i(\boldsymbol{kB})s_z &= -i\frac{m\zeta}{r} + \frac{B_z}{r}\frac{d}{dr}(rs_r).\end{aligned} \quad (25)$$

Then, using Equations (22) and excluding s_φ and s_z by means of Equation (25), from Equation (15) follows

$$\begin{aligned}K = \frac{1}{4\pi}\Bigg[&\left(k^2 + \frac{m^2}{r^2}\right)\\ &\times\left(\zeta + \frac{ikB_\varphi(ds_r/dr - s_r/r) - im(B_z/r)(ds_r/dr + s_r/r)}{k^2 + m^2/r^2}\right)^2\\ &+ \left((\boldsymbol{kB})^2 - \frac{2}{r^2}B_\varphi\frac{d}{dr}(rB_\varphi)\right)s_r^2 + B_z^2\left(\frac{ds_r}{dr} + \frac{s_r}{r}\right)^2\\ &+ B_\varphi^2\left(\frac{ds_r}{dr}\frac{s_r}{r}\right)^2\\ &- \frac{[kB_\varphi(ds_r/dr - s_r/r) - (mB_z/r)(ds_r/dr + s_r/r)]^2}{k^2 + m^2/r^2}\Bigg].\end{aligned} \quad (26)$$

This expression has the minimum value at

$$\zeta = -\frac{i}{k^2 + (m/r)^2}\left[\left(kB_\varphi - \frac{m}{r}B_z\right)\frac{ds_r}{dr} - \left(kB_\varphi + \frac{m}{r}B_z\right)\frac{s_r}{r}\right], \quad (27)$$

and Equation (26) reduces to

$$\begin{aligned}K = \frac{1}{4\pi}\Bigg[&\frac{[(\boldsymbol{kB})(ds_r/dr) + hs_r/r]^2}{k^2 + m^2/r^2}\\ &+ \left((\boldsymbol{kB})^2 - \frac{2}{r^2}B_\varphi\frac{d}{dr}(rB_\varphi)\right)s_r^2\Bigg],\end{aligned} \quad (28)$$

where

$$h = kB_z - \frac{m}{r}B_\varphi.$$

Therefore, in accordance with Equations (14) and (28), the minimization procedure leads to the following (see also Newcomb 1960)

$$\begin{aligned}W_j = \frac{L}{16\pi}\int_{S_j}\Bigg\{&\frac{(r(\boldsymbol{kB})(ds_r/dr) + hs_r)^2}{k^2r^2 + m^2}\\ &+ \frac{s_r^2}{r^2}\left(r^2(\boldsymbol{kB})^2 - 2B_\varphi\frac{d}{dr}(rB_\varphi)\right)\Bigg\}2\pi r dr,\end{aligned} \quad (29)$$

where the lower index j corresponds to i and e. The first two terms under the integral (29) are positively determined and stabilize the instability development. Therefore, only the last term, which is related to the the longitudinal current j_z, can be responsible for the instability.

After integration of the term with $s_r ds_r/dr$ from Equation (29) we obtain the following expression for potential energy inside a flux rope

$$\begin{aligned}W_i &= \frac{L}{8}\int_0^a\left(f_i\left(\frac{ds_r}{dr}\right)^2 + g_i s_r^2\right)dr + W_a,\\ W_a &= \frac{L}{8}\frac{k^2a^2B_{zi}^2(a) - m^2B_\varphi^2(a)}{k^2a^2 + m^2}s_r^2(a),\end{aligned} \quad (30)$$

where

$$f_i = r\frac{(krB_{zi} + mB_\varphi)^2}{k^2r^2 + m^2},$$
$$g_i = \frac{1}{r}\frac{(krB_{zi} - mB_\varphi)^2}{k^2r^2 + m^2} + \frac{1}{r}(krB_{zi} + mB_\varphi)^2 - \frac{2B_\varphi}{r}\frac{d}{dr}(rB_\varphi) - \frac{d}{dr}\left(\frac{k^2r^2B_{zi}^2 - m^2B_\varphi^2}{k^2r^2 + m^2}\right).$$

Note that the last equation by means of the equilibrium (i.e., Equation (18)) can be reduced to the expression obtained previously by Shafranov (1970)

$$g_i = \frac{8\pi k^2r^2}{k^2r^2 + m^2}\frac{dp}{dr} + \frac{(krB_{zi} + mB_\varphi)^2}{r}\frac{k^2r^2 + m^2 - 1}{k^2r^2 + m^2} + \frac{2k^2r}{(k^2r^2 + m^2)^2}(k^2r^2B_{zi}^2 - m^2B_\varphi^2). \quad (31)$$

The potential energy outside a flux rope is

$$W_e = \frac{L}{8}\int_a^\infty \left(f_e\left(\frac{ds_r}{dr}\right)^2 + g_e s_r^2\right)dr + W_{ae},$$
$$W_{ae} = \frac{L}{8}\frac{k^2a^2B_{ze}^2(a)}{k^2a^2 + m^2}s_r^2(a), \quad (32)$$

where

$$f_e = r\frac{(krB_{ze})^2}{k^2r^2 + m^2},$$
$$g_e = k^2B_{ze}^2 r\left(1 + \frac{k^2r^2 - m^2}{(k^2r^2 + m^2)^2}\right).$$

Equations (30)–(32) at $k^2a^2 \ll 1$ and $m \neq 0$ reduce to the form

$$W_a = \frac{L}{8}\frac{k^2a^2B_{zi}^2(a) - m^2B_\varphi^2(a)}{m^2}s_r^2(a),$$
$$f_i = r\frac{(krB_{zi} + mB_\varphi)^2}{m^2},$$
$$g_i = \frac{8\pi k^2r^2}{m^2}\frac{dp}{dr} + \frac{(krB_{zi} + mB_\varphi)^2(k^2r^2 + m^2 - 1)}{rm^2} + 2\frac{k^2r}{m^4}(k^2r^2B_{zi}^2 - m^2B_\varphi^2),$$
$$W_{ae} = \frac{L}{8}\frac{k^2a^2B_{ze}^2(a)}{m^2}s_r^2(a),$$
$$f_e = r\frac{(krB_{ze})^2}{m^2},$$
$$g_e = k^2B_{ze}^2 r\frac{m^2 - 1}{m^2}. \quad (33)$$

The kink ($m = 1$) mode of the magnetic flux rope should be most unstable since $g_i \propto m^2$ at $m \to \infty$ (see the Appendix and Miyamoto 1988 for the particular case of homogeneous current).

4. The Eigenfunctions

In order to find the expressions for eigenfunctions we should find solutions of the Euler–Lagrange equations (see e.g., Shafranov 1970):

$$\frac{d}{dr}\left(f_i\frac{ds_r}{dr}\right) - g_i s_r = 0, \quad r \leqslant a, \quad (34)$$
$$\frac{d}{dr}\left(f_e\frac{ds_r}{dr}\right) - g_e s_r = 0, \quad r > a, \quad (35)$$

which have to satisfy the matching conditions at $r = a$.

By using Equations (33) and taking into account that the external magnetic field $B_{ze} = \text{const}$, from Equation (35) we obtain

$$\frac{1}{r}\frac{d}{dr}\left(r^3\frac{ds_r}{dr}\right) + (1 - m^2)s_r = 0. \quad (36)$$

The solution of differential Equation (36), which describes displacement s_r outside of the flux rope, is

$$s_r = s_r(a)\left(\frac{a}{r}\right)^{m+1}. \quad (37)$$

For the kink mode ($m = 1$), the solution (37) reduces to (see also Cheremnykh et al. 2017)

$$s_r = s_r(a)\left(\frac{a}{r}\right)^2, \quad r > a, \quad (38)$$

and will be used in the next section.

According to Equations (33) and (34), the equation for s_r inside the flux rope in the long-wavelength limit, e.g., $ka \ll 1$, takes the following form

$$\frac{1}{r}\frac{d}{dr}\left(r^3(\boldsymbol{kB}_i)^2\frac{ds_r}{dr}\right) + (1 - m^2)(\boldsymbol{kB}_i)^2 s_r = 0. \quad (39)$$

It should be stressed that the points where $\boldsymbol{kB}_i = 0$ are usually called resonant points (Shafranov 1970).

For the kink mode from Equation (39) it follows that

$$\frac{d}{dr}\left(r^3(\boldsymbol{kB}_i)^2\frac{ds_r}{dr}\right) = 0. \quad (40)$$

When the singular points are absent ($\boldsymbol{kB}_i \neq 0$) the trivial solution of Equation (40) can be represented as (see also Bahari & Khalvandi 2017; Cheremnykh et al. 2017)

$$s_r = s_0 = \text{const}, \; r \leqslant a. \quad (41)$$

Note that in the Equation (30), the term proportional to ds_r/dr under the integral sign is equal to zero in this case.

To determine the condition of the absence of resonant points let us rewrite Equation (40) in the following form

$$\frac{d}{dr}\left[r^3\left(\frac{\Phi(r)}{2\pi} - n\right)^2\frac{ds_r}{dr}\right] = 0, \quad \Phi(r) = \frac{LB_\varphi(r)}{rB_{zi}(r)}, \quad n = -\frac{Lk}{2\pi}. \quad (42)$$

If $\Phi(r)$ is a monotonously decreasing function of r and by taking into account that the minimum value of $n = 1$, the resonant point inside the magnetic flux tube is absent at

$$\frac{\Phi(r = 0)}{2\pi} < 1,$$

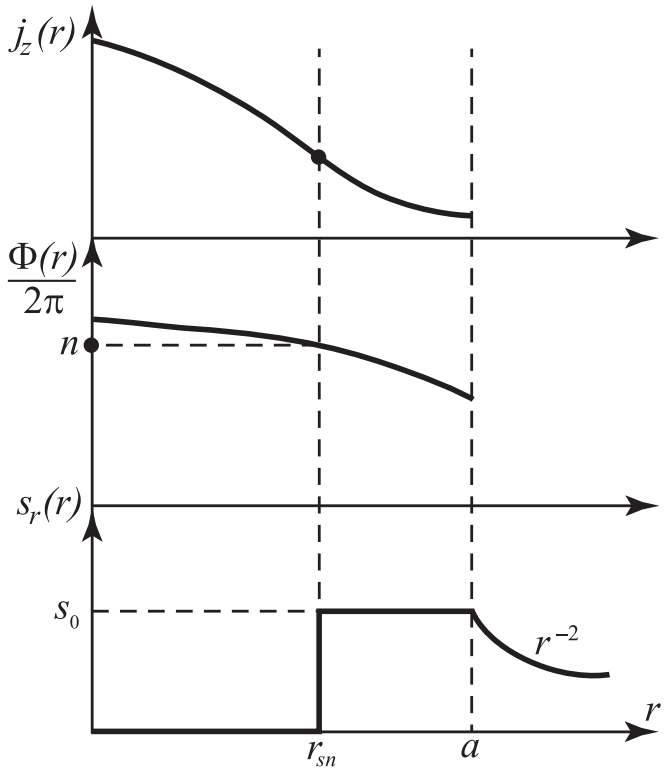

Figure 2. The schematic plots of the resonant point and solution shown in Equation (43).

and, therefore, the resonance effects can be ignored (see also Cheremnykh et al. 2017).

For the general case, when the resonant point r_{sn} inside the magnetic flux rope is present, from Equation (42) it is easy to show that the expression for W_i can be minimized if

$$s_r = \begin{cases} 0, & 0 \leqslant r \leqslant r_{sn}, \\ s_0, & r_{sn} < r \leqslant a. \end{cases} \tag{43}$$

The behavior of function (43), as well as resonant points r_{sn} determined by expression

$$\frac{\Phi(r = r_{sn})}{2\pi} = n,$$

are shown in Figure 2. Under such a choice of s_r the contribution of the term, which is proportional to f_i under the sign of integral (30), vanishes at $r \to r_{sn}$.

5. The Stability of the Kink Mode

Let us obtain the expression for the total potential energy W at $m = 1$ by assuming the arbitrary distribution of the current $j(r)$ over the cross section of the magnetic flux rope. By substituting solution (38) into Equation (32), the potential energy outside a flux rope can be represented as

$$W_e = \frac{L}{8} k^2 a^2 B_{ze}^2 s_r^2(a). \tag{44}$$

As it follows from Equations (21) and (44), the values of W_σ and W_e are positive and, therefore, the external and surface perturbations should stabilize the development of kink instability, which can be associated only with the internal potential energy W_i.

Since the term with f_i under the sign of integral for W_i in Equation (30) should be negligibly small and

$$\frac{L}{8} \frac{s_0^2}{W_a} \int_{r_{sn}}^{a} g_i dr \sim k^2 a^2, \tag{45}$$

it is easy to see that in the long-wavelength limit $W_i \approx W_a$. Note that the relationship (45) is satisfied in the case of a few resonant points inside of the magnetic flux rope.

Hence, in view of Equations (21), (33), and (44)

$$W = W_a + W_e + W_\sigma = \frac{L}{8} k^2 a^2 s_r^2(a)(B_{zi}^2 + B_{ze}^2) > 0, \tag{46}$$

where $B_{zi} = B_{zi}(a)$. Thus, the magnetic flux rope will remain stable in respect to the kink modes for arbitrary values of twist angles Φ in the long-wavelength limit.

In accordance with Equation (A3)

$$\int_{V_i} \rho \boldsymbol{s}^2 dV + \int_{V_e} \rho \boldsymbol{s}^2 dV = (\rho_i + \rho_e) s_r^2(a) \pi a^2 L, \tag{47}$$

and from Equations (13) and (46) the square of eigenfrequencies for a flux rope is

$$\Omega^2 = \frac{k^2}{4\pi} \frac{B_{zi}^2 + B_{ze}^2}{(\rho_i + \rho_e)}. \tag{48}$$

Equation (48) coincides with numerical and analytical results obtained previously by Bennett et al. (1999) and Cheremnykh et al. (2017), respectively. However, we did not impose any restriction on the dependence of the longitudinal B_{zi} component (i.e., on j_φ current component) on r whereas according to Bennett et al. (1999) and Cheremnykh et al. (2017) it should be constant.

Equation (48) also coincides with the dispersion relation for the untwisted thin magnetic flux tube (e.g., Spruit 1982; Roberts et al. 1984; Tsap & Kopylova 2001). This equation was proposed by Nakariakov & Ofman (2001) to determine the absolute value of the magnetic field strength $B^{\rm ut}$ in untwisted coronal loops at low plasma beta $\beta = 8\pi p/B^2 \ll 1$. The authors have shown that the transverse magnetic loop oscillations can be related to the global (fundamental) standing kink modes. By using the equation of the pressure balance, $B^{\rm ut} = B_{zi}^{\rm ut} = B_{\rm ze}$, the corrected calculated formula (there is a typo in Equation (6) of Nakariakov & Ofman 2001) has the form (see also Aschwanden 2004; Nakariakov & Verwichte 2005):

$$B^{\rm ut} = B_{zi}^{\rm ut} = \sqrt{8\pi} \frac{L}{T} \sqrt{\rho_i (1 + \rho_e/\rho_i)}, \tag{49}$$

where T is the observed period of transverse oscillations. For the typical magnetic loop parameters the estimated magnetic field $B^{\rm ut}$ turned out to be equal to 4–30 G (see, e.g., Nakariakov & Ofman 2001; Nakariakov & Verwichte 2005). Equation (49) provides us the value of the magnetic field in an assumption that no magnetic twist is present.

As it follows from our analysis the dispersion relation (48) can also be used for magnetic field diagnostics of twisted coronal loops. In fact, the equation of the pressure balance at the boundary $r = a$ in case of $\beta \ll 1$ in accordance with the Equation (16) can be written as

$$(B^{\rm tw})^2 = B_\varphi^2 + (B_{zi}^{\rm tw})^2 = B_{\rm ze}^2. \tag{50}$$

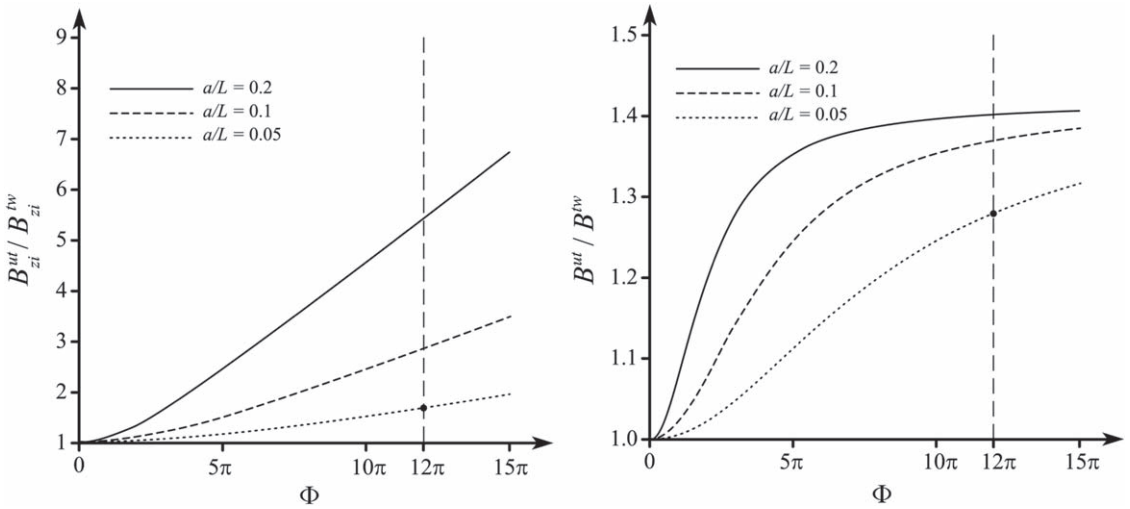

Figure 3. The dependence of ratios for longitudinal (B_{zi}^{ut}/B_{zi}^{tw}) and absolute (B^{ut}/B^{tw}) magnetic fields of untwisted (ut) and twisted (tw) flux tubes on the total twist angle Φ. The vertical dashed line corresponds to the observed twist angle of the loop $\Phi = 12\pi$ as reported by Srivastava et al. (2010).

The phase velocity Ω/k for the fundamental mode is $\Omega/k = 2L/T$. Since $B_\varphi = B_{zi}^{tw}\Phi a/L$ with regard for Equations (48) and (50), the longitudinal magnetic field component of the twisted magnetic flux tube can be represented as

$$B_{zi}^{tw} = \frac{4L}{T}\sqrt{\frac{\pi\rho_i(1+\rho_e/\rho_i)}{2+(a/L\Phi)^2}}. \quad (51)$$

Equations (49) and (51) provide

$$\frac{B_{zi}^{ut}}{B_{zi}^{tw}} = \sqrt{\frac{2+(a/L\Phi)^2}{2}}. \quad (52)$$

By using Equations (50) and (51), the estimate of the absolute value of the magnetic field strength for the twisted magnetic flux tube can be found as

$$B^{tw} = \frac{4L}{T}\sqrt{\pi\rho_i(1+\rho_e/\rho_i)}\sqrt{\frac{1+(a/L\Phi)^2}{2+(a/L\Phi)^2}}. \quad (53)$$

Therefore, according to Equations (49) and (53), the ratio between B^{ut} and B^{tw} is a function of the total twist angle Φ and can be represented as

$$\frac{B^{ut}}{B^{tw}} = \sqrt{2}\sqrt{\frac{1+(a/L\Phi)^2}{2+(a/L\Phi)^2}}. \quad (54)$$

The dependence of ratios for longitudinal (B_{zi}^{ut}/B_{zi}^{tw}) and absolute (B^{ut}/B^{tw}) magnetic fields as the function of angle Φ calculated by using Equations (52) and (54) for the aspect ratios $a/L = 0.05$, 0.1, and 0.2 are presented in Figure 3. It is clearly seen that these ratios depend on Φ significantly. Following observational results reported by Srivastava et al. (2010), for the estimated twist angle $\Phi \approx 12\pi$ and the aspect ratio $a/L = 0.05$, from Equations (52) and (54) it follows that $B_{zi}^{ut}/B_{zi}^{tw} \approx 1.67$ and $B^{ut}/B^{tw} \approx 1.28$.

6. Discussion and Conclusions

In the present paper, the kink stability of a shielding magnetic flux rope with a surface current has been studied. This type of magnetic configuration may be generated, for example, by the vortex plasma motions (see, e.g., Kitiashvili et al. 2012, 2013; Giagkiozis et al. 2018; Snow et al. 2018; Murawski et al. 2018) accompanied by the slight penetration of magnetic field lines into the external region due to the ohmic diffusion. At the same time, the questions on physical mechanisms responsible for generation of surface neutralized and nonneutralized electric currents remain open (e.g., Dalmasse et al. 2015; Georgoulis 2018; Schmieder & Aulanier 2018).

We have used an energy principle approach which allowed us to analyze the general properties of kink and other MHD modes in the presence of surface current and obtain the exact expressions for eigenfunctions and eigenvalues which usually can be found by using the normal modes method. Following Parker (1996) we limited our study to the model of a magnetic flux rope with a surface current shielding the azimuthal component of magnetic field outside the tube. In particular, an energy principle permitted us to generalize results obtained by Cheremnykh et al. (2017) and conclude that surface currents may stabilize the kink ($m = 1$) and fluting ($m > 1$) modes under coronal conditions in the long-wavelength limit. This result is independent of the radial profile of the current density. It supports a number of flare models which include connection of the energy release with nonneutralized electric currents (e.g., Kliem & Török 2006; Stepanov & Zaitsev 2016).

The calculated estimates suggest that kink modes should be dominant under coronal conditions since a minimal amount of energy is needed for their generation. In particular, it explains the ubiquitous character of decayless kink oscillations in the solar corona (see, e.g., Nisticò et al. 2013; Anfinogentov et al. 2015). We have also shown that the dispersion relation (48), which is often used for the magnetic field diagnostics in untwisted coronal loops, remains true for twisted ones.

Our findings also indicate that surface currents may play a significant role in the dynamics of magnetic flux tubes. The detection of these currents is an important practical task as they may completely stabilize the development of kink instability. New high-resolution spatial observations of the dynamic magnetic field by the Daniel K. Inouye Solar Telescope should be very helpful for a better understanding of this process.

Y.T., A.S., and Y.K. were partially supported by the Russian Foundation for Basic Research (project No.18-02-00856) and the Ministry of Education and Science (project No. 0831-2019-0006).

O.C. and A.K. would like to thank the Integrated Scientific Programmes of National Academy of Sciences of Ukraine on Plasma Physics and Space Research for partial support. V.F. is grateful to The Royal Society, International Exchanges Scheme, collaboration with Brazil and Chile (IES191114); Science and Technology Facilities Council (STFC) grant ST/M000826/1. Also, V.F. would like to thank the International Space Science Institute (ISSI) in Bern, Switzerland, for the hospitality provided to the members of the team on "The Nature and Physics of Vortex Flows in Solar Plasmas." This research has received financial support from the European Union's Horizon 2020 research and innovation program under grant agreement No. 824135 (SOLARNET).

Appendix
Homogeneous Current

For the uniform longitudinal current density ($j_z = \text{const}$) the azimuthal magnetic field according to Ampere's law (5) has the following form:

$$B_\varphi(r) = B_\varphi(a)\frac{r}{a}.$$

Therefore, the solution of the differential Equation (39) described displacements inside a flux rope can be represented as:

$$s_r = s_r(a)\left(\frac{r}{a}\right)^{m-1}. \tag{A1}$$

Substituting Equation (A1) into Equation (30) we obtain that the potential energy of internal perturbations is

$$W_i = \frac{s_r(a)^2 L}{8m^2}[(kaB_{zi} + mB_\varphi(a))^2(m-1) + k^2a^2B_{zi}^2 - m^2B_\varphi^2(a)]. \tag{A2}$$

If plasma densities inside ρ_i and outside ρ_e of a flux rope are slowly varying functions of r, we find

$$\int_{V_i}\rho \mathbf{s}^2 dV + \int_{V_e}\rho \mathbf{s}^2 dV = \frac{\rho_i+\rho_e}{m}s_r^2(a)\pi a^2 L. \tag{A3}$$

As a result, from Equations (13), (21), (A2), and (A3) we get the square of eigenfrequencies for a flux rope with the uniform electric current density j_z in the long-wavelength limit:

$$\Omega^2 = \frac{1}{4\pi(\rho_i+\rho_e)}\left[k^2(B_{zi}^2+B_{ze}^2) + \frac{2k}{a}(m-1)B_zB_\varphi(a) + \frac{m(m-1)}{a^2}B_\varphi^2(a)\right]. \tag{A4}$$

Equation (A4) coincides with the corresponding equation obtained by Cheremnykh et al. (2017) using the method of normal modes and the dispersion relation (48) at $m = 1$. In addition, from Equation (A4) it follows that the excitation of eigenmode with $m = 1$ will be accompanied by the minimum potential energy change.

ORCID iDs

Yuriy Tsap https://orcid.org/0000-0001-5074-7514
Viktor Fedun https://orcid.org/0000-0002-0893-7346
Oleg Cheremnykh https://orcid.org/0000-0001-6789-3382

References

Anfinogentov, S. A., Nakariakov, V. M., & Nisticò, G. 2015, A&A, 583, A136
Aschwanden, M. J. 2004, Physics of the Solar Corona. An Introduction (Praxis Publishing: Chichester)
Bahari, K., & Khalvandi, M. R. 2017, SoPh, 292, 192
Bennett, K., Roberts, B., & Narain, U. 1999, SoPh, 185, 41
Bernstein, I. B., Frieman, E. A., Kruskal, M. D., & Kulsrud, R. M. 1958, RSPSA, 244, 17
Chen, J. 2017, PhPl, 24, 090501
Cheremnykh, O., Fedun, V., Ladikov-Roev, Y., & Verth, G. 2018, ApJ, 866, 86
Cheremnykh, O. K., Fedun, V., Kryshtal, A. N., & Verth, G. 2017, A&A, 604, A62
Dalmasse, K., Aulanier, G., Démoulin, P., et al. 2015, ApJ, 810, 17
Dungey, J. W. 2016, Cosmic Electrodynamics (Cambridge: Cambridge Univ. Press)
Fan, Y. 2009, LRSP, 6, 4
Georgoulis, M. K. 2018, in Electric Currents in Geospace and Beyond, ed. A. Keiling, O. Marghitu, & M. Wheatland (Washington, DC: American Geophysical Union), 371
Giagkiozis, I., Fedun, V., Scullion, E., Jess, D. B., & Verth, G. 2018, ApJ, 869, 169
Goedbloed, J. P. H., & Poedts, S. 2004, Principles of Magnetohydrodynamics (Cambridge: Cambridge Univ. Press)
Hassanin, A., Kliem, B., & Seehafer, N. 2016, AN, 337, 1082
Hood, A. W. 1986, SoPh, 103, 329
Hood, A. W., & Priest, E. R. 1981, GApFD, 17, 297
Kitiashvili, I. N., Kosovichev, A. G., Lele, S. K., Mansour, N. N., & Wray, A. A. 2013, ApJ, 770, 37
Kitiashvili, I. N., Kosovichev, A. G., Mansour, N. N., Lele, S. K., & Wray, A. A. 2012, PhyS, 86, 018403
Kliem, B., & Török, T. 2006, PhRvL, 96, 255002
Kruskal, M., & Schwarzschild, M. 1954, RSPSA, 223, 348
Leontovich, M. A., & Shafranov, V. D. 1961, in Plasma Physics and the Problem of Controlled Thermonuclear Reactions, ed. M. A. Leontovich (New York: Pergamon), 255
Linton, M. G., Longcope, D. W., & Fisher, G. H. 1996, ApJ, 469, 954
Liu, J., Wang, Y., & Erdélyi, R. 2019, FrASS, 6, 44
Melrose, D. B. 1991, ApJ, 381, 306
Melrose, D. B. 1995, ApJ, 451, 391
Melrose, D. B. 1996, ApJ, 471, 497
Melville, J. P., Hood, A. W., & Priest, E. R. 1986, SoPh, 105, 291
Mikic, Z., Schnack, D. D., & van Hoven, G. 1990, ApJ, 361, 690
Miyamoto, K. 1988, PPCF, 30, 1493
Murawski, K., Kayshap, P., Srivastava, A. K., et al. 2018, MNRAS, 474, 77
Myers, C. E., Yamada, M., Ji, H., et al. 2015, Natur, 528, 526
Nakariakov, V. M., & Ofman, L. 2001, A&A, 372, L53
Nakariakov, V. M., Ofman, L., Deluca, E. E., Roberts, B., & Davila, J. M. 1999, Sci, 285, 862
Nakariakov, V. M., & Verwichte, E. 2005, LRSP, 2, 3
Newcomb, W. A. 1960, AnPhy, 10, 232
Nisticò, G., Nakariakov, V. M., & Verwichte, E. 2013, A&A, 552, A57
Parker, E. N. 1979, AstQ, 3, 201
Parker, E. N. 1996, ApJ, 471, 485
Priest, E., & Forbes, T. 2000, Magnetic Reconnection: MHD Theory and Applications (New York: Cambridge Univ. Press)
Priest, E. R. 1984, Solar Magneto-hydrodynamics (Dordrecht: Reidel)
Roberts, B., Edwin, P. M., & Benz, A. O. 1984, ApJ, 279, 857
Russell, A. J. B., Demoulin, P., Hornig, G., Pontin, D. I., & Candelaresi, S. 2019, ApJ, 884, 55
Ryutov, D. A., & Ryutova, M. P. 1976, JETP, 43, 491
Ryutova, M. 2018, Physics of Magnetic Flux Tubes (Cham: Springer)
Sakurai, T. 1976, PASJ, 28, 177
Schmieder, B., & Aulanier, G. 2018, in Electric Currents in Geospace and Beyond, ed. A. Keiling, O. Marghitu, & M. Wheatland, 235 (Washington, DC: American Geophysical Union), 391
Shafranov, V. D. 1970, SPTP, 15, 175
Snow, B., Fedun, V., Gent, F. A., Verth, G., & Erdélyi, R. 2018, ApJ, 857, 125
Spruit, H. C. 1981, A&A, 98, 155
Spruit, H. C. 1982, SoPh, 75, 3
Srivastava, A. K., Zaqarashvili, T. V., Kumar, P., & Khodachenko, M. L. 2010, ApJ, 715, 292

Stepanov, A. V., & Zaitsev, V. V. 2016, Ge&Ae, 56, 952
Török, T., & Kliem, B. 2005, ApJL, 630, L97
Tsap, Y. T., & Kopylova, Y. G. 2001, AstL, 27, 737
Tsap, Y. T., Kopylova, Y. G., & Stepanov, A. V. 2006, ARep, 50, 1026
Tsap, Y. T., Kopylova, Y. G., Stepanov, A. V., Melnikov, V. F., & Shibasaki, K. 2008, SoPh, 253, 161
Tsap, Y. T., Stepanov, A. V., & Kopylova, Y. G. 2018, Ge&Ae, 58, 942
Weber, M. A., & Browning, M. K. 2016, ApJ, 827, 95
Wheatland, M. S. 2000, ApJ, 532, 616
Wilkinson, L. K., Emslie, A. G., & Gary, G. A. 1992, ApJL, 392, L39
Zagorodny, A., & Cheremnykh, O. 2014, Introduction to the Plasma Physics (Kiev: Naukova Dumka), 696